Spatial Selectivity of Rice Channel Based on 3-D Joint Multipath Shape Factors Theory

Derong Du[1, 3, a], Yueqin Chen[1, b], Linlin Jiang[1, c], Ziyao Ding[1, d], Long Li[2, *], Xiaoping Zeng[3, e]

[1] School of Electronic Information Engineering, Yangtze Normal University, 408100 Chongqing, China.

[2] Guangxi Key Laboratory of Trusted Software, Guilin University of Electronic Technology, 541004 Guilin, China.

[3] School of Microelectronics and Communication Engineering, Chongqing University, 400044 Chongqing, China.

* Corresponding author: lilong@guet.edu.cn, [a]Derongdu2022@163.com, [b]yueqinchen2022@163.com, [c]linlinjiang2022@163.com, [d]ziyaoding2022@163.com, [e]xiaopingzeng2022@163.com

Abstract. Based on the 3-D joint multipath shape factors theory, this paper studies the spatial selectivity of Rice channels of wireless communications. A 3-D joint multipath angular power spectral density (APD) model is proposed, and then the closed expressions of the 3-D double spherical harmonic coefficients and 3-D joint multipath shape factors are derived. The errors in the existing formulas of 3-D joint multipath shape factors theory are further pointed out and corrected. The results can provide theoretical support for quantifying and simplifying the analysis and design of 3-D multiple input multiple output (MIMO) beamforming technology and smart antenna arrays for the 5G communication.

Keyword: 3-D joint, wireless communication, rate spectral density (APD) model.

1. Introduction

Electromagnetic waves in different paths have dissimilar propagation delays [1], and the fading rates to the receiving ends are different. The spatial selectivity of multipath fading impacts on the performance of the communication system [2].[1] and [3] proposed the concept of multipath fading, introduced channel fading in detail, introduced first-order and second-order small-scale fading channels. [4] put forward the 2-D theory of multipath shape factors, derived 2-D complex spherical harmonic function, spatial parameters. [5] compared the essential scattering models of spatial channel measurement, and proposed a spatial channel model based on fading statistics. In order to study the spatial characteristics of line-of-sight (LoS) and non-LoS (NLoS) channels, a measurement-based 24 GHz wave propagation in city and suburban scenarios was proposed in [6].

[7] further summarized the theory of multipath shaping factor on the basis of [4], and established a 3-D APD model. Based on the 3-D APD, six non-normative complex spherical harmonic functions, spatial parameters and fading rate variance were derived. In [8], the characteristic equations of the first and second moments of the directional dispersion, spatial selectivity of the wireless channel and the analysis results of the correlation between the two moments were presented. [9] defined and described the spatial covariance matrix of the second-order moments of directional energy distribution through analysis of the second-order moments of spatial fading. [10] derived a 3-D APD model in which the LoS and NLoS radio wave arrives from the transmitter to the receiver with equal probability. [11] established two 3-D multipath APD models for Rice channel, and analyzed the fading rate variance, level passing rate, average fading period and spatial correlation function. [12] proposed the theory of 2-D and 3-D joint shape factors. [13] proposed a geometrically generalized and coordinated 3-D random model, derived the analytical expression of the direction angle in the 3-D joint channel.

Owing to flexibility and suitability, the Rician fading is often used to model the wireless propagation comprising a LoS component and a scattered NLoS component. This paper strives to alleviate the current lack of analytical studies, and the contributions and novelties of this paper are summarized as follows.

(1) A 3-D multipath APD model is proposed for the spatial selectivity analysis of Rician channel considering both receiving and transmitting ends;

(2) The double spherical harmonic coefficients and shaping factors are derived based on the proposed APD;

(3) Some errors of existing joint shape factors theory formulas in [12] and [13] are pointed out and corrected.

(4) The analysis results will provide help for the design of 3D joint MIMO beamforming technology and smart antenna array for 5G communications [14] [15].

2. 3-D APD Model and joint multipath shape factors

2.1 Joint Multipath Shape Factors Theory

For the 3-D channel, joint multipath shape factors can be derived based on the l-th order m-th order and k-th order p-order double spherical harmonic coefficients $S_{l,k}^{m,p}$ of the 3-D APD [12].

$$S_{l,k}^{m,p}=\int_0^{2\pi}\int_{-\frac{\pi}{2}}^{\frac{\pi}{2}}\int_0^{2\pi}\int_{-\frac{\pi}{2}}^{\frac{\pi}{2}} p(\theta_{\mathrm{T}},\varphi_{\mathrm{T}},\theta_{\mathrm{R}},\varphi_{\mathrm{R}})Y_{l,k}^{m,p^*}\cos\varphi_{\mathrm{T}}\cos\varphi_{\mathrm{R}}\,d\theta_{\mathrm{T}}d\varphi_{\mathrm{T}}d\theta_{\mathrm{R}}d\varphi_{\mathrm{R}}, \tag{1}$$

where θ_{T} and φ_{T} represent the azimuthal and elevational angles of the transmitting end respectively, and θ_{R} and φ_{R} represent the azimuthal and elevational angles of the receiving end respectively. $Y_{l,k}^{m,p}$ is the double spherical harmonic function.

2.2 3-D Joint APD Model

The 3-D joint APD model is proposed as follows:

$$\begin{aligned}P(\theta_{\mathrm{T}},\varphi_{\mathrm{T}},\theta_{\mathrm{R}},\varphi_{\mathrm{R}}) &= P(\theta_{\mathrm{T}},\varphi_{\mathrm{T}})\,P(\theta_{\mathrm{R}},\varphi_{\mathrm{R}})\\ &= \frac{P_{\mathrm{T}}P_{\mathrm{R}}}{4\pi^4(K+1)^2}\left[1+2\pi^2K\delta(\theta_{\mathrm{T}}-\theta_0,\varphi_{\mathrm{T}}-\varphi_0)\right]\left[1+2\pi^2K\delta(\theta_{\mathrm{R}}-\theta_1,\varphi_{\mathrm{R}}-\varphi_1)\right],\end{aligned} \tag{2}$$

where P_{T} is the total signal power transmitted at the transmitting end, P_{R} is the total signal power received at the receiving end, K is the Rician K-factor, $f_{\mathrm{NLoS}}(,)=1/2\pi^2$ is the probability density of the NLoS waves of transmitting or receiving end, $f_{\mathrm{LoS}}(,)$ is the probability density of the LoS waves of transmitting or receiving end, $\delta(,)$ is the 2-D Dirac delta function used to describe $f_{\mathrm{LoS}}(,)$.

2.3 Double spherical harmonic coefficients

According to [12], some $Y_{l,k}^{m,p}$ we already know, and we can infer other $Y_{l,k}^{m,p}$ as follows:

$$\begin{aligned}&Y_{0,1}^{0,0}(\theta,\varphi)=\sin\varphi_{\mathrm{R}},\ Y_{0,1}^{0,1}(\theta,\varphi)=\cos\varphi_{\mathrm{R}}e^{j\theta_{\mathrm{R}}},\ Y_{0,2}^{0,0}(\theta,\varphi)=2\sin^2\varphi_{\mathrm{R}}-2/3,\\ &Y_{0,2}^{0,1}(\theta,\varphi)=\sin 2\varphi_{\mathrm{R}}e^{j\theta_{\mathrm{R}}},\ Y_{0,2}^{0,2}(\theta,\varphi)=\cos^2\varphi_{\mathrm{R}}e^{j2\theta_{\mathrm{R}}},\ Y_{1,1}^{0,1}(\theta,\varphi)=\cos\varphi_{\mathrm{R}}e^{j\theta_{\mathrm{R}}}\sin\varphi_{\mathrm{T}},\\ &Y_{0,1}^{0,-1}(\theta,\varphi)=\cos\varphi_{\mathrm{R}}e^{-j\theta_{\mathrm{R}}}.\end{aligned} \tag{3}$$

But, $Y_{2,0}^{0,0}(\theta,\varphi)$ and $Y_{2,0}^{1,0}(\theta,\varphi)$ in (3) proposed by [17] are not correct, and they should be corrected to

$$Y_{2,0}^{0,0}(\theta,\varphi)=\sin^2\varphi_{\mathrm{T}}-1/3,Y_{2,0}^{1,0}(\theta,\varphi)=1/2\sin\varphi_{\mathrm{T}}e^{j\theta_{\mathrm{T}}}. \tag{4}$$

In addition, $Y_{0,2}^{0,0}(\theta,\varphi)$ and $Y_{0,2}^{0,1}(\theta,\varphi)$ also should be corrected to

$$Y_{0,2}^{0,0}(\theta,\varphi)=\sin^2\varphi_{\mathrm{R}}-1/3, Y_{0,2}^{0,1}(\theta,\varphi)=1/2\sin\varphi_{\mathrm{R}}e^{j\theta_{\mathrm{R}}}. \tag{5}$$

Double spherical harmonic coefficients $S_{l,k}^{m,p}$ can be derived as follows:

$$\begin{aligned}
&S_{0,0}^{0,0}=\frac{P_TP_R}{\pi^2(K+1)^2}(2+\pi K\cos\varphi_0)(2+\pi K\cos\varphi_1), S_{1,0}^{0,0}=\frac{P_TP_R}{2\pi(K+1)^2}K(2+\pi K\cos\varphi_1)\sin 2\varphi_0,\\
&S_{0,1}^{0,0}=\frac{P_TP_R}{2\pi(K+1)^2}K(2+\pi K\cos\varphi_0)\sin 2\varphi_1, S_{1,1}^{0,0}=\frac{P_TP_R}{4(K+1)^2}K^2\sin 2\varphi_0\sin 2\varphi_1,\\
&S_{1,1}^{1,0}=\frac{P_TP_R}{2(K+1)^2}K^2e^{-j\theta_0}\cos^2\varphi_0\sin 2\varphi_1, S_{1,1}^{0,1}=\frac{P_TP_R}{2(K+1)^2}K^2e^{-j\theta_1}\cos^2\varphi_1\sin 2\varphi_0,\\
&S_{1,0}^{1,0}=\frac{P_TP_R}{\pi(K+1)^2}Ke^{-j\theta_0}(2+\pi K\cos\varphi_1)\cos^2\varphi_0, S_{0,1}^{0,1}=\frac{P_TP_R}{\pi(K+1)^2}Ke^{-j\theta_1}(2+\pi K\cos\varphi_0)\cos^2\varphi_1,\\
&S_{1,1}^{1,1}=\frac{P_TP_R}{(K+1)^2}K^2e^{-j(\theta_0+\theta_1)}\cos^2\varphi_0\cos^2\varphi_1, S_{1,1}^{1,-1}=\frac{P_TP_R}{(K+1)^2}K^2e^{j(\theta_1-\theta_0)}\cos^2\varphi_0\cos^2\varphi_1,\\
&S_{2,0}^{0,0}=\frac{P_TP_R}{3\pi(K+1)^2}K(3\sin^2\varphi_0-1)(2+\pi K\cos\varphi_1)\cos\varphi_0, S_{0,2}^{0,0}=\frac{P_TP_R}{3\pi(K+1)^2}K(3\sin^2\varphi_1-1)(2+\pi K\cos\varphi_0)\cos\varphi_1,\\
&S_{2,0}^{1,0}=\frac{P_TP_R}{\pi(K+1)^2}Ke^{-j\theta_0}(2+\pi K\cos\varphi_1)\sin\varphi_0\cos^2\varphi_0, S_{0,2}^{0,1}=\frac{P_TP_R}{\pi(K+1)^2}Ke^{-j\theta_1}(2+\pi K\cos\varphi_0)\sin\varphi_1\cos^2\varphi_1,\\
&S_{2,0}^{2,0}=\frac{P_TP_R}{\pi(K+1)^2}K\mathrm{e}^{-j2\theta_0}(2+\pi K\cos\varphi_1)\cos^3\varphi_0, S_{0,2}^{0,2}=\frac{P_TP_R}{\pi(K+1)^2}K\mathrm{e}^{-j2\theta_1}(2+\pi K\cos\varphi_0)\cos^3\varphi_1,\\
&S_{0,1}^{0,-1}=\frac{P_TP_R}{\pi(K+1)^2}Ke^{j\theta_1}(2+\pi K\cos\varphi_0)\cos^2\varphi_1.
\end{aligned} \tag{6}$$

2.4 3-D Joint Shape Factors

The APD of the 3-D joint forming factor has been established above, and complex spherical harmonics have been derived. The shaping factors of the three-dimensional channel are 4.9-4.19 of the paper [12], but the formula 4.15 of the paper [12] is not rigorous, and it is hereby corrected.

$$\Xi=\frac{2\left(S_{1,1}^{0,0}S_{0,0}^{0,0}-S_{1,0}^{0,0}S_{0,1}^{0,0}\right)}{2S_{0,0}^{0,0^2}-\left(S_{1,0}^{0,0^2}+S_{0,1}^{0,0^2}+\left|S_{1,0}^{1,0}\right|^2+\left|S_{0,1}^{0,1}\right|^2\right)}=0. \tag{7}$$

3. Results and discussions

This section uses MATLAB to simulate the 3-D joint APD and effect of LoS direction and Rician K-factor on joint shape factors for the general urban communication scenarios in the 2.4 GHz frequency band. Due to some 3-D joint shape factors are equal to zero, they are no longer analyzed in this section. In addition, some incorrect formulas mentioned above in [12] and [13] also are confirmed through simulation. For ease of analysis, the total transmitting power is normalized, i.e., PT=1 in simulations.

3.1 3-D Joint APD

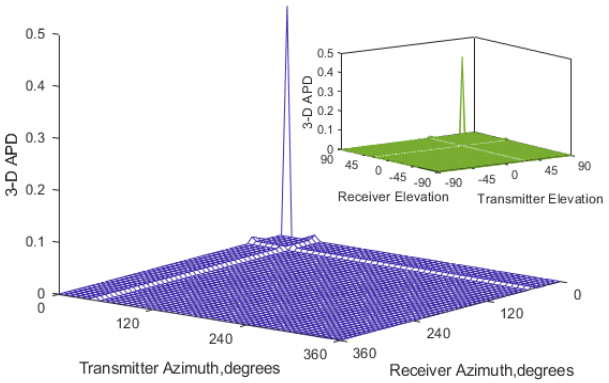


Figure 1. The 3-D joint APD of the Rician channel.

Fig. 1 illustrates the 3-D joint APD of the Rician channel for different directions. The values of the simulation parameters used in this section are set to K=2, azimuth and elevation in LoS direction are pi/4, and pi/6 respectively. For ease of presentation, the 3-D joint APDs are given from the azimuth direction and the elevation direction respectively. As shown in Fig. 1, the 3-D joint APD reaches the maximum at $(\pi/4, \pi/6)$, which is the direction of LoS. This is because powers in angles of arrival and departure of NLoS waves are evenly distributed in 3-D sphere space, and the probability density of the LoS waves is modeled as the 2-D Dirac delta function.

3.2 Effect of LoS Direction on Joint Shape Factors

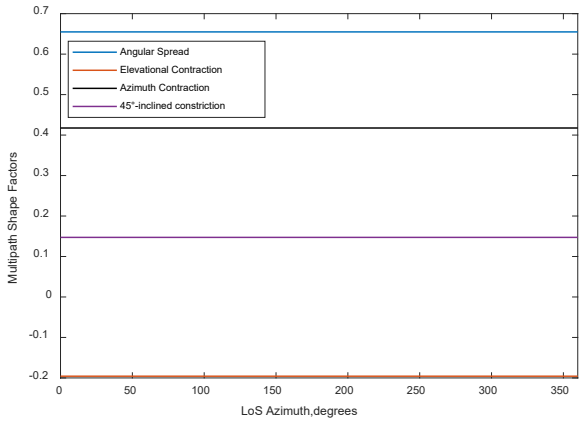


Figure 2. The joint shape factors in the LoS azimuth direction.

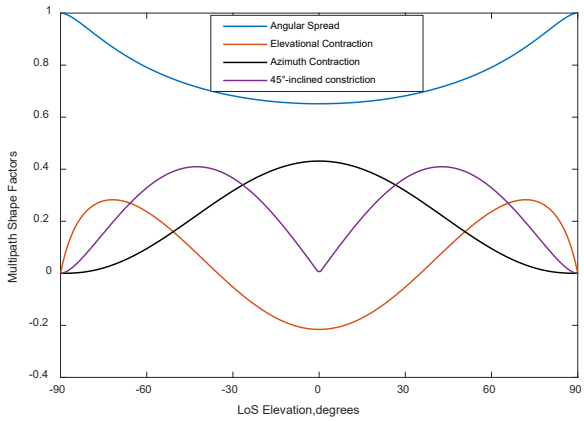


Figure 3. The joint shape factors in the LoS elevation direction.

Fig. 2 illustrates the joint shape factors in the LoS azimuth direction. The values of the simulation parameters used in Fig. 2 are set to K=2, and elevation in LoS direction is pi/18. As shown in Fig.2, the angular spread, elevational constriction, azimuthal constriction and 45°-inclined constriction are constants, indicating that they are not affected by the LoS azimuthal direction. In detail, the angular spread is approximately equal to 0.7, indicating that the small-scale fading is very small; 45°-inclined constriction is equal to -0.2, indicating that the two diameters are concentrated in the elevational angle direction, and the azimuthal angle has almost no effect. Azimuthal contraction is the degree of concentration of the two diameter directions in the azimuthal angle direction, and it is equal to 1 means that the two diameters are concentrated in the elevational angle direction.

Fig. 3 illustrates the joint shape factors in the LoS elevation direction. The values of the simulation parameters used in Fig. 2 are set to K=2, and azimuth in LoS direction is pi/4. As shown in Fig. 3, all the curves of the angular spread, elevational constriction, azimuthal constriction and 45°-inclined constriction are symmetrical at the elevation of 0°. If elevation is equal to 0, joint shape factors are

equal to 0.6, -0.2, 0.4 and 0 respectively. At the same time, azimuthal constriction gets the maximum value, and angular spread, elevational constriction and 45°-inclined constriction get the minimum values. It should be noted that elevational constriction and 45°-inclined constriction have multiple maximum or minimum values. In the direction of LoS elevation, the angular spread starts to fade from 1, the lowest point equals to 0.6, and then it returns to 1. If the angular spread equals to 1, it indicates that the channel has no multipath fading. If the angular spread is from 1 to 0.6, it indicates that there is no obvious small-scale fading. The elevational contraction increases from 0 to 0.3 and then begins to decrease to -0.2, and it gets larger values in the direction of LoS elevation [-90°, -60°] and [60°, 90°], indicating the channel fading is small. The azimuth contraction first increases from 0 to 0.4 and then drops to 0, indicating that the two diameters come from the same elevational angle direction. The 45°-inclined angle contraction starts to rise from 0, the highest point is 0.4, and then the lowest point is 0.

3.3 Effect of Rician K-factor on Joint Shape Factors

Fig. 4 illustrates the joint shape factors with different Rician K-factors. The values of the simulation parameters used in this section are set to azimuth and elevation in LoS direction are pi/4, and pi/18 respectively. The Rician K-factor is defined as the ratio of the power of the LoS signal to the power of the NLoS component, and its value directly reflects the degree of channel fading. If the K-factor's value is small, it means the channel fading is serious, and its value is large, the opposite is true. As shown in Fig.4, with the increase of K-factor, angular spread, elevational constriction, azimuthal constriction and 45°-inclined constriction are gradually approaching a constant. With the increase of K-factor, angular spread and elevational constriction gradually decrease, but the angular spread decays more quickly, indicating the multipath power is no longer concentrated on a certain direction angle, which has a greater impact on the quality of channels. The azimuthal constriction and 45°-inclined constriction gradually increase at an approximate rate. In the end, the angular spread and 45°-inclined constriction tend to 0.2, azimuthal constriction tends to 0.4, and elevational contraction tends to -0.2. When the K-factor reaches a certain value, it no longer has effect on the joint shape factors, implying that the channel fading is already very small.

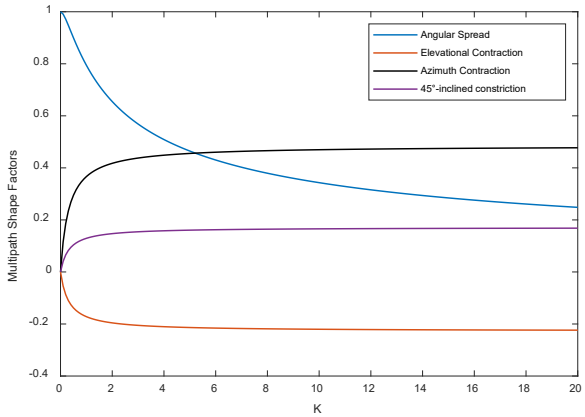


Figure 4. The joint shape factors with different Rician K-factors.

4. Conclusion

The performance of many 5G communication technologies including 3-D MIMO beamforming technology and smart antenna arrays is closely related to the 3-D spatial selectivity of multipath fading. This paper proposes a 3-D joint multipath APD model for the Rice channel. Based on the APD, the closed expressions of the 3-D double spherical harmonic coefficients and 3-D joint multipath shape factors are derived. The errors in the existing formulas of 3-D joint multipath shape factors theory are further pointed out and corrected. The simulation analysis shows that the 3-D spatial angular directions have significant effect on fading statistics of Rician channel.

Acknowledgments

This work was sponsored by Natural Science Foundation of Chongqing, China (No. cstc2019jcyj-msxmX0821), Science and Technology Research Program of Chongqing Municipal Education Commission (Grant No. KJQN201901418, KJQN202101437), Guangxi Key Laboratory of Trusted Software (No. kx202015).

References

[1] Theodore S. Rappaport, "Wireless Communications Principles and Practice," Publishing house of electronic industry, American, pp.122-123, Dec. 2001.

[2] D. Du, X. Zeng and X. Jian,"Analysis of 3-D Spatial selectivity for Rician Channel," Radioengineering, vol. 27, no. 1, PP. 249-255, Apr. 2018.

[3] G. D. Durgin, "Space-Time Wireless Channels," American, Prentice Hall, pp.30-102, Oct. 2002.

[4] G. D. Durgin and T. S. Rappaport, "Theory of multipath shape factors for small-scale fading wireless channels," IEEE Transactions on Antennas and Propagation, vol. 48, no. 5, pp. 82-693, May 2000.

[5] Z. M. Loni and N. M. Khan, "Analysis of fading statistics in cellular mobile communication systems," The Journal of Supercomputing, vol. 64, no. 2, p. 295–309, Jun. 2013.

[6] I. Rodriguez, E. P. L. Almeida, R. Abreu, M. Lauridsen, A. Loureiro and P. Mogensen, "Analysis and comparison of 24 GHz cm Wave radio propagation in urban and suburban scenarios," in Proc. IEEE Wireless Communications and Networking Conference, Doha, Qatar, pp. 1-7, Apr. 2016.

[7] D. G. Valchev and D. Brady, "Three-dimensional multipath shape factors for spatial modeling of wireless channels," IEEE Transactions on Wireless Communications, vol. 8, no. 11, pp. 5542-5551, Nov. 2009.

[8] B. H. Fleury, "First- and second-order characterization of direction dispersion and space selectivity in the radio channel," IEEE Transactions on Information Theory, vol. 46, no. 6, pp. 2027-2044, Sep. 2000.

[9] A. Pal, M. Beach and A. Nix, "A Novel Quantification of 3D Directional Spread from Small-Scale Fading Analysis," in Proc. IEEE International Conference on Communications, Istanbul, Turkey, pp. 1699-1704, Jun. 2006.

[10] R. H. Clarke and Wee Lin Khoo, "3-D mobile radio channel statistics," IEEE Transactions on Vehicular Technology, vol. 46, no. 3, pp. 798-799, Aug. 1997.

[11] D. Du, "Research on Models of the 3D Channel and Interference of Vehicle-to-Vehicle Communications," Chongqing University, Jun. 2018.

[12] D. G. Valchev,"Spatial modeling of three-dimensional multipath wireless channels," Northeastern University, Aug. 2008.

[13] A. Ahmed, S. J. Nawaz, S. M. Gulfam, S. Wyne, M. N. Patwary and H. Pervaiz, "Angular Spread Quantification of Multi-Antenna Vehicular Radio Communication Channels," in Proc. IEEE Globecom Workshops (GC Wkshps), Abu Dhabi, United Arab, pp. 1-7, Dec. 2018.

[14] H. W. Yuan, G. F. Cui, and J. Fan, "A Method for Analyzing Broadcast Beamforming of Massive MIMO Antenna Array," Progress In Electromagnetics Research Letters, Vol. 65, 15-21, 2017.

[15] Mohamed Hadi Habaebi, Mohanad Janat, and Md. Rafiqul Islam, "Beam Steering Antenna Array for 5G Telecommunication Systems Applications," Progress In Electromagnetics Research M, Vol. 67, 197-207, 2018.